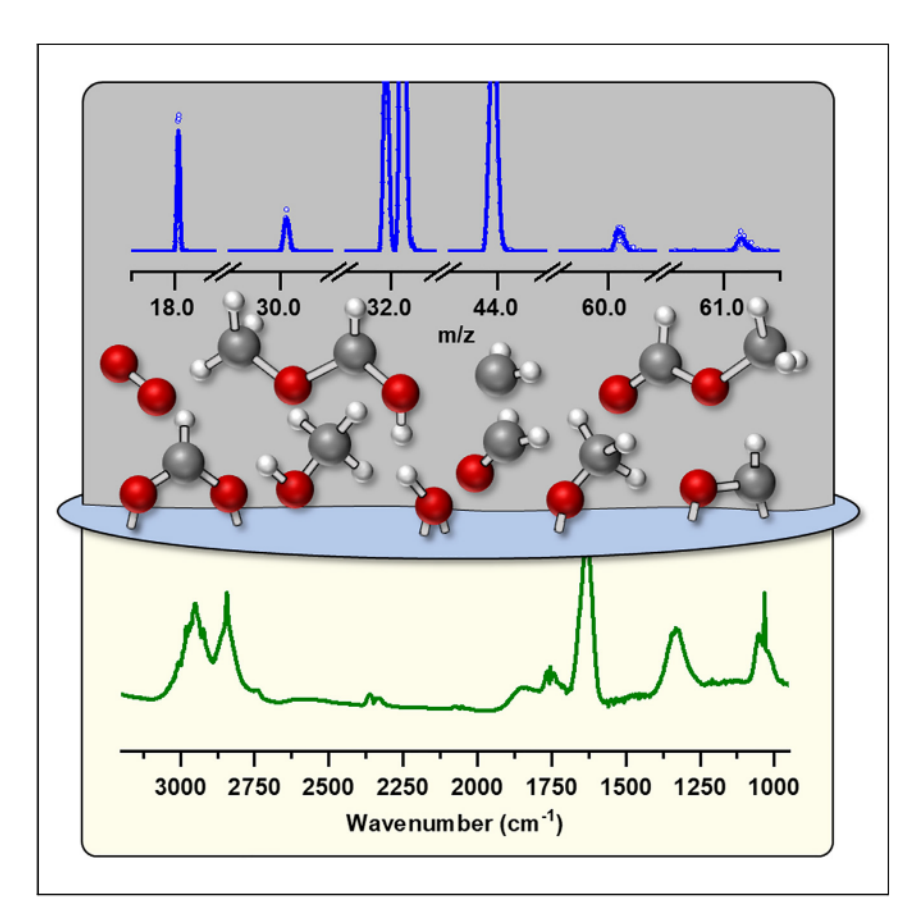


### **Article**

Constraining reaction pathways for methanol oxidation through operando interrogation of both the surface and the near-surface gas phase



During a heterogeneous catalytic reaction, unique information about the reaction mechanism can be obtained when chemical events and species both on the surface and in the near-surface gas phase are studied. This is true for methanol oxidation to upgraded products, where valuable information on the role of surface-bound formaldehyde is deduced through observations made on both regions.

Sadi M. Gurses, Noah Felvey, Leah R. Filardi, ..., David L. Osborn, Nils Hansen, Coleman X. Kronawitter

ckrona@ucdavis.edu

### Highlights

The near-surface gas phase contains useful information about heterogeneous reactions

The composition of the nearsurface gas phase is a reporter of events on the surface

During methanol oxidation, the fate of formaldehyde controls key reaction pathways

MgO-supported  $PdO_x$  is a useful model system for understanding methanol oxidation catalysis



Gurses et al., Chem Catalysis 3, 100782 October 19, 2023 © 2023 Elsevier Inc. https://doi.org/10.1016/j.checat.2023.100782





### **Article**

# Constraining reaction pathways for methanol oxidation through operando interrogation of both the surface and the near-surface gas phase

Sadi M. Gurses,<sup>1</sup> Noah Felvey,<sup>1</sup> Leah R. Filardi,<sup>1</sup> Angie J. Zhang,<sup>2</sup> Joseph Wood,<sup>3</sup> Klaus van Benthem,<sup>3</sup> Jonathan H. Frank,<sup>2</sup> David L. Osborn,<sup>1,2</sup> Nils Hansen,<sup>2</sup> and Coleman X. Kronawitter<sup>1,4,\*</sup>

### **SUMMARY**

We combine near-surface molecular beam mass spectrometry—a probe of the gas phase within hundreds of micrometers of catalyst surfaces—and surface-sensitive infrared spectroscopy to study methanol oxidation at atmospheric pressure with the use of MgOsupported PdOx. The study of adsorbate and near-surface gasphase compositions under reaction conditions suggests that the fate of surface-generated CH<sub>2</sub>O—its desorption, its spillover, and its reaction with surface oxygenates—is central to C<sub>2</sub> product generation. However, the reactivity of CH<sub>2</sub>O prevents its observation on surfaces. The key support for the mechanistic claim originates from observations of gas-phase methoxymethanol, which is too reactive for detection by traditional techniques: this molecule contains the dioxymethylene group, implicating a methylene-containing intermediate in the initial coupling event. This work shows that probes of the near-surface region yield information complementary to that obtained through surface-sensitive spectroscopy. Their combined use is an underexplored, yet powerful, strategy for developing and constraining reaction pathways for catalysis.

### INTRODUCTION

Operando surface-sensitive spectroscopy that probes the identities of molecular adsorbates contributes essential information toward discovering the reaction mechanisms of heterogeneous catalytic systems. The data obtained from the use of this tool are made more impactful when combined with product identification in reactor effluents; thereby, specific surface adsorbates can be correlated with reaction outcomes. However, the primary products of heterogeneous reactions—those species that desorb from catalyst surfaces—might undergo chemical transformation from subsequent interactions with the catalyst, the reactor wall surfaces, or the downstream experimental apparatus and are thus often not reflected in reactor effluent analyses even when care is taken to operate in regimes of differential conversion where secondary reactions are minimized. For some reactions, primary products are too reactive or unstable to be detected by conventional analysis tools. In many cases, investigators will be unaware of the presence of reactive or unstable primary products in the gas phase unless an interrogation tool with the required detection selectivity is applied. Examples of this include high-temperature reactions that release radicals into the gas phase (e.g., alkyl and hydroxyl radicals during oxidative dehydrogenation or coupling of alkanes<sup>3,4</sup> and hydrogen radicals during direct dehydrogenation of alkanes). 5 Conversion of simple alcohols occurs at comparably low temperatures, yet can also produce a variety of highly reactive species, including

### THE BIGGER PICTURE

We obtain impactful information about heterogeneous reactions by correlating chemical events and species on catalyst surfaces with reaction outcomes. However, for many systems, the molecules desorbing into the near-surface gas phase are not the same as those detected in reactor effluents; they might be too reactive to exist there. Here, we combine measurements of the surface and near-surface gas phase and report insights unavailable from interrogation of only one of those regions. We study methanol oxidation with the use of MgO-supported PdO<sub>x</sub> catalysts. Under conditions selective for C<sub>2</sub> product generation, surface-sensitive measurements indicate the presence of methoxy and formate adsorbates. However, detection in the near-surface gas phase of abundant methoxymethanol—a species too reactive to be detected by traditional techniques—and its associated chemical structure provide evidence that formaldehyde, undetected on the surface but transiently present, is the key intermediate for the reaction.





# Chem Catalysis Article

closed-shell oxygenates<sup>6</sup> and radicals<sup>7</sup> that exist only transiently in conventional reactor beds. For these and many other systems, it is useful to consider, by analogy with the goals of *operando* tools to analyze solids, that the near-surface gas phase contains reaction fingerprints that can similarly contribute mechanistic inputs.<sup>6–9</sup>

Here we analyze both the surface and the near-surface gas phase during oxidative conversion of methanol with MgO-supported Pd. In this study, the phrase "near-surface" refers to the gas-phase region within several millimeters of the catalyst surface. Near-surface molecular beam mass spectrometry (ns-MBMS)<sup>7</sup> is used as a universal detector of species at a position 500 µm above the surface of the packed catalyst powder, and diffuse reflectance infrared Fourier transform spectroscopy (DRIFTS) is used to track the vibrational signatures of adsorbates. We show that when the species compositions of the two phases are correlated, the mechanisms derived from these correlations are uniquely constrained by capture of elusive intermediates in the gas phase. Specifically, our approach facilitates the study of near-surface methoxymethanol (CH<sub>3</sub>OCH<sub>2</sub>OH), which is a reactive intermediate species generated by heterogeneous catalytic methanol oxidation whose reaction/decomposition precludes its detection through conventional tools such as gas chromatography, but which we have recently detected and analyzed by ns-MBMS.<sup>6</sup> One of our most important observations is that methyl formate (CH<sub>3</sub>OCHO) and methoxymethanol desorb as products concurrently for all conditions examined, suggesting they share a mechanistic connection. This connection is understood through interpretation of surface-sensitive DRIFTS measurements: whereas under reaction conditions the catalyst surface is densely populated with methoxy (CH<sub>3</sub>O) and formate (HC(O)O) species in a variety of bonding configurations, the presence of the dioxymethylene (O-CH<sub>2</sub>-O) group in near-surface methoxymethanol requires that formaldehyde (CH<sub>2</sub>O), undetected on the surface but transiently present, be the primary building block of the C<sub>2</sub> oxygenates.

### **RESULTS**

### Approach to interrogating both the surface and the near-surface gas phase

Figure 1 provides an overview of the approach used in this study. Figure 1A shows representative operando DRIFTS spectra, and the right panel shows ns-MBMS data, sampled through a quartz microprobe at a fixed position 500 µm above the surface of the packed catalyst powders. The insets show online mass spectrometry data recorded from the effluent of the DRIFTS reactor cell (hard ionization using a conventional quadrupole spectrometer at 70 eV electron energy), which were periodically recorded to confirm that the identities of evolved products during DRIFTS matched those found by ns-MBMS. Details of the ns-MBMS apparatus for heterogeneous catalysis are provided in a recent publication, and an updated diagram of the setup is provided in Figure S1. The measurements for this study were recorded in a reactor that utilizes a stagnation flow configuration, <sup>10</sup> as shown schematically at the top of Figure 1B. Use of stagnation flow simplifies the flow profile in the near-surface region: reactant and product diffusion occur in a 1D boundary layer perpendicular to the packed catalyst surface. The stagnation flow configuration is not particularly relevant to this study, except that it provides highly reproducible flow conditions and minimizes radial concentration gradients.

As shown in the representative data in Figure 1, the MgO-supported Pd catalyst system was investigated through independent measurements with samples preoxidized by  $O_2$  (PdO/MgO), mixed-valent samples pre-oxidized and reduced with  $H_2$  (Pd-PdO/MgO), and the bare MgO support (see the supplemental information

<sup>&</sup>lt;sup>1</sup>Department of Chemical Engineering, University of California, Davis, Davis, CA 95616, USA

<sup>&</sup>lt;sup>2</sup>Combustion Research Facility, Sandia National Laboratories, Livermore, CA 94551, USA

<sup>&</sup>lt;sup>3</sup>Department of Materials Science & Engineering, University of California, Davis, Davis, CA 95616, USA

<sup>&</sup>lt;sup>4</sup>Lead contact

<sup>\*</sup>Correspondence: ckrona@ucdavis.edu https://doi.org/10.1016/j.checat.2023.100782

**Article** 



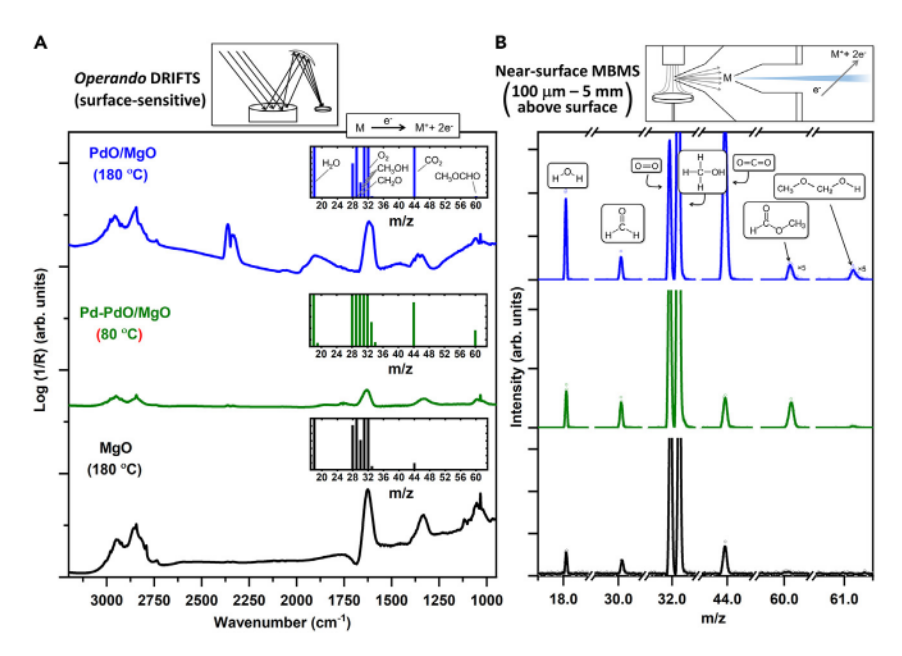


Figure 1. Overview of approach to studying methanol oxidation over MgO-supported Pd catalysts, illustrated with representative DRIFTS and ns-MBMS data

From top to bottom, data are shown for pre-oxidized samples (PdO/MgO), pre-oxidized and reduced samples (Pd-PdO/MgO), and the bare MgO support.

(A) DRIFTS spectra at respective temperatures of activity. Insets: mass spectra periodically recorded online from cell effluent (70 eV).

(B) Mass spectra from ns-MBMS (500  $\mu$ m above surface) with species identified (17 eV). Open circles represent data, and lines represent smoothing. The peaks used for tracking the molecules in this study are indicated; they correspond to (parent molecule, monitored cation, m/z) water, H<sub>2</sub>O<sup>+</sup>, 18.01; formaldehyde, CH<sub>2</sub>O<sup>+</sup>, 30.01; methanol, CH<sub>3</sub>OH<sup>+</sup>, 32.03; dioxygen, O<sub>2</sub><sup>+</sup>, 31.99; carbon dioxide, CO<sub>2</sub><sup>+</sup>, 43.99; methyl formate, C<sub>2</sub>H<sub>4</sub>O<sub>2</sub><sup>+</sup>, 60.02; and methoxymethanol, monitored at fragment ion C<sub>2</sub>H<sub>5</sub>O<sub>2</sub><sup>+</sup>, 61.03.

for information on treatments). This sample naming scheme is based on conclusions from catalyst characterization, discussed below. The strategy outlined here facilitates interpretation of surface adsorbate compositions in the context of near-surface gas-phase speciation, and vice versa. The reflectron time-of-flight spectrometer has mass resolution m/ $\Delta m = 3,500,^{11}$  which, along with the use of tunable energies (nominally 8–20 eV) for soft electron ionization, enables identification of products and reactive intermediates through simultaneous measurement of isotopologues as well as energy-dependent fragment ion signals, which serve as fingerprints of parent molecules (reactants, intermediates, and products). The species analyzed in this study are identified in the high-resolution mass spectra in Figure 1: methanol (CH<sub>3</sub>OH), dioxygen (O<sub>2</sub>), water (H<sub>2</sub>O), carbon dioxide (CO<sub>2</sub>), formaldehyde (CH<sub>2</sub>O), methyl formate (CH<sub>3</sub>OCHO), and methoxymethanol (CH<sub>3</sub>OCH<sub>2</sub>OH).

The chemical states of Pd in the catalysts used in this study were analyzed by X-ray photoelectron spectroscopy (XPS; Figure 2) at the Pd 3d level. Pd 3d spectra in general contain two prominent peaks, which originate from spin orbit splitting of the Pd 3d level: ca. 334–340 eV (3d<sub>5/2</sub>) and ca. 340–345 eV (3d<sub>3/2</sub>). For the sample calcined at 700°C in an  $O_2$ /He mixture, the largest contribution to the Pd 3d<sub>5/2</sub> peak, with 337.2 eV center energy, indicates the presence of Pd<sup>2+</sup>. <sup>12–14</sup> There is an additional contribution by a peak at 335.5 eV, which originates from Pd<sup>0</sup>. <sup>12</sup> Figure S2 provides an X-ray diffractogram that shows the presence of PdO crystallites in this sample, which is consistent with the observation of primarily Pd<sup>2+</sup> through XPS;



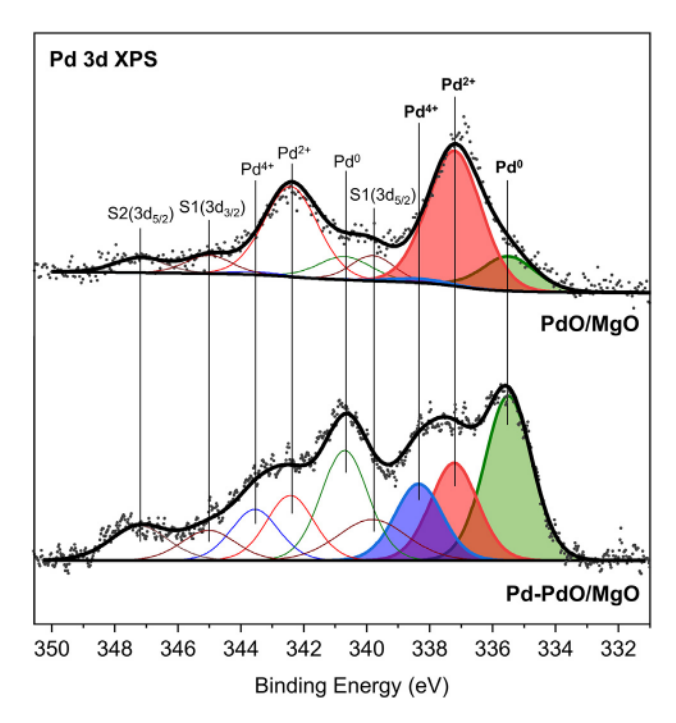


Figure 2. X-ray photoelectron spectra for the catalysts used in this study PdO/MgO refers to the catalyst calcined at 700°C in  $O_2$ /He; Pd-PdO/MgO refers to the catalyst calcined at 700°C in  $O_2$ /He and then reduced in  $H_2$  at 300°C. The radiation source is Mg K $\alpha$  (1,253.6 eV). Spectra are normalized.

consequently, this sample is referred to as PdO/MgO throughout this study. After subsequent reduction in H<sub>2</sub> at 300°C, the intensity distribution in the associated XPS spectrum (Figure 2) is altered. The most prominent contribution to the  $3d_{5/2}$ peak is centered at 335.5 eV, which is consistent with reduction to Pd<sup>0</sup>. Additional intensity near 338.3 eV is also evident after reduction, which has previously been assigned to Pd with a higher oxidation state. 15 High-valent Pd, such as Pd4+, 16 has been observed in MgO-supported Pd, 17 and it has been noted that PdO2 can be stabilized through the interaction of cationic Pd with oxide supports. 14 Given this mixed-valent character, this sample is referred to as Pd-PdO/MgO throughout this study. The additional peaks required for the deconvolution of the remaining peaks in the Pd 3d spectra ( $3d_{3/2}$  and satellite peaks) all have physical origins and are well documented. The three contributions to the  $3d_{5/2}$  peak, discussed above, are associated with three 3d<sub>3/2</sub> peaks at 5.2 eV higher binding energy.<sup>18</sup> Satellite S1 peaks (339.8 and 345.0 eV) have been studied previously and hypothesized to be related to crystal field or multiplet effects associated with Pd<sup>2+15</sup> and are centered at a binding energy 2.6 eV greater than Pd2+ peaks. Satellite S2, which has been reported to originate from a charge transfer process in palladium oxides, 15 is measured here to be centered at 347.2 eV.

A representative high-angle annular dark-field scanning transmission electron microscopy (HAADF-STEM) image of the PdO/MgO sample is provided in Figure S3. Bright intensities in the HAADF-STEM image reveal that the MgO particles support faceted PdO crystallites with an average particle size of approximately 30 nm. HAADF-STEM micrographs recorded from Pd-PdO/MgO samples reveal no detectable particle sintering during reduction.

**Article** 



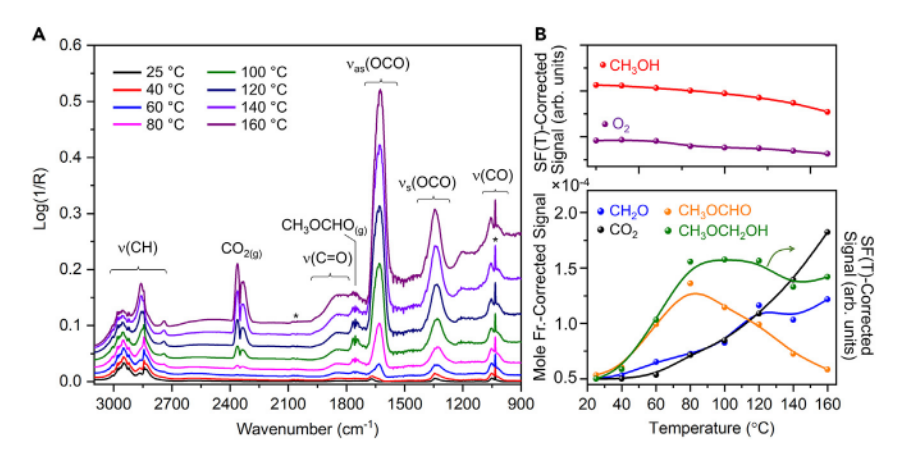


Figure 3. Operando surface and near-surface characterization of Pd-PdO/MgO during methanol oxidation

Spectra were recorded between 25°C and 160°C;  $p_{\text{CH}_3\text{OH}}/p_{\text{O}_2} = 1.45$ . \*Gas-phase methanol peak. (A) DRIFTS results; spectral regions characteristic of major vibrational modes are labeled. (B) ns-MBMS results (500  $\mu$ m above surface) for reactants (top) and products (bottom). Lines were added to guide the eyes.

### Methanol oxidation with MgO-supported Pd

#### Pd-PdO/MgO catalysts

Oxide-supported Pd catalysts are commonly used for methanol oxidation,  $^{19,20}$  and reaction outcomes can depend on the initial chemical state of the material. For example, pre-reduction of Pd/Al $_2$ O $_3$  catalysts in H $_2$  has been shown to dramatically increase low-temperature activity and selectivity toward methyl formate.  $^{21}$  Using the combined surface-near-surface characterization methodology discussed above, we examined the pre-reduced MgO-supported Pd powder (Pd-PdO/MgO) as a methanol oxidation catalyst between 25°C and 160°C. Figure 3A shows the temperature dependence of DRIFTS spectra recorded during methanol oxidation with a CH $_3$ OH/O $_2$  feed ratio of 1.45. The top of Figure 3A contains labels describing the general character of vibrational modes within the spectral regions where features are observed to evolve with increasing temperature. In these and all other operando methanol oxidation spectra in this article, a spectrum recorded on the catalyst powder in He flow prior to introduction of reactants was used as the background.

Figure 3B provides the results of ns-MBMS measurements with the sampling probe positioned 500  $\mu$ m above the packed Pd-PdO/MgO powder. In this figure, all species' signals have been corrected to account for gas temperature, <sup>7</sup> and stable products (CO<sub>2</sub>, CH<sub>3</sub>OCHO, and CH<sub>2</sub>O) have been calibrated to adjust for the species' associated instrument detection efficiencies<sup>6</sup> (see the supplemental information for a calibration description). These calibrated signals are referred to as "mole-fraction corrected," and their ratios quantify product mole-fraction ratios.

The integrated signals plotted in Figure 3B are proportional to reactant and product mole fractions in the near-surface region. If we take these results together with the Fourier transform infrared (FTIR) spectra of Figure 3A, it is possible to interpret the appearance and temperature-dependent concentrations of products released from the surface in the context of surface adsorbate compositions. At a high level, it is apparent from the FTIR spectra that with increasing temperature: (1) the intensities of peaks in the  $\nu_{as}(OCO)$  (centered near 1,630 cm<sup>-1</sup>) and  $\nu_{s}(OCO)$  (centered near 1,330 cm<sup>-1</sup>) regions grow, (2) the relative intensities of peaks in the  $\nu$ (CH) regions (2,700–3,100 cm<sup>-1</sup>) evolve and some new minor peaks appear, (3)  $\nu$ (C=O)



# Chem Catalysis Article

peaks (1,800–2,000 cm $^{-1}$ ) grow, and (4) the signatures of gas-phase species (CO<sub>2(g)</sub> [2,348 cm $^{-1}$ ] and CH<sub>3</sub>OCHO<sub>(g)</sub> [1,752 cm $^{-1}$ ]) become evident. It is known from many prior methanol oxidation studies that the wavenumbers for the  $\nu_{as}(\text{OCO})$  and  $\nu_{s}(\text{OCO})$  modes observed here correspond to those of surface-bound formates  $^{22}$  (HC(O)O<sub>(s)</sub>; throughout this article, the subscript "(s)" refers to surface-bound species). The absorption in the  $\nu(\text{CH})$  region reflects contributions from all adsorbed species with C–H bonds, including CH<sub>3</sub>OH<sub>(s)</sub>, methoxy (CH<sub>3</sub>O<sub>(s)</sub>), and HC(O)O<sub>(s)</sub>. The spectral features centered near 1,050 cm $^{-1}$  are associated with  $\nu(\text{CO})$  modes of CH<sub>3</sub>OH<sub>(s)</sub> (1,050 cm $^{-1}$ ), CH<sub>3</sub>O<sub>(s)</sub> (monodentate, 1,111 cm $^{-1}$ ; bidentate 1,090 cm $^{-1}$ ), and CH<sub>3</sub>OH<sub>(g)</sub> (1,033 cm $^{-1}$ ). The broad  $\nu(\text{C=O})$  peaks can definitively be assigned to Pd–CO<sub>(s)</sub> with contributions from both linearly and bridge-bonded CO<sub>(s)</sub>.

During the temperature ramp, the Pd-PdO/MgO catalyst initiates methanol oxidation activity between 25°C and 40°C, a low temperature that is consistent with those reported in prior studies of pre-reduced oxide-supported Pd catalysts.<sup>21</sup> This low-temperature activity creates challenges in establishing relationships between surface and near-surface compositions. For example, at 60°C, a temperature at which CO<sub>2</sub>, CH<sub>2</sub>O, CH<sub>3</sub>OCHO, and CH<sub>3</sub>OCH<sub>2</sub>OH are all released to the nearsurface gas phase (Figure 3B), it is clear that the surface is populated with a mixture of  $CH_3O_{(s)}$ ,  $HC(O)O_{(s)}$ , and  $CO_{(s)}$  (assigned through the signatures noted in the previous paragraph). There is no clear evidence of adsorbed formaldehyde or methylene-containing species, which can be observed on oxides at low temperatures,<sup>22</sup> despite observation of their presence in the near-surface gas phase. Although the data of Figure 3 do facilitate such general observations, the spectral features associated with adsorbates on Pd-PdO/MgO are broad and unresolved, and they are present for essentially the entire temperature range examined. Therefore, the precise bonding configurations of adsorbates cannot be determined from these data, and furthermore, their appearances cannot be selectively correlated with those of gas-phase species. For example, it is known that multiple bonding configurations contribute intensity to the v(OCO) modes of formate, <sup>26</sup> but the formate peaks in Figure 3A are broad and symmetrical, and these contributions are not distinguishable.

### PdO/MgO catalysts

The freshly oxidized catalyst PdO/MgO was also examined as a methanol oxidation catalyst via the combined surface-near-surface investigative approach. In contrast to the observations made for Pd-PdO/MgO above, the DRIFTS spectra collected during methanol oxidation with PdO/MgO (Figure 4A) contain highly spectrally resolved features (that is, the contributions to absorption feature line shapes are resolved and can be deconvolved). In addition, the temperature dependencies of changes to spectra were much more evident. The catalysts are stable under the conditions examined: after reaction at the highest temperature used (180°C), XPS spectra indicate no change from that associated with the initial as-prepared catalyst (Figure S4).

High-temperature calcination of oxides in oxygen environments increases the degree of crystallinity (structural uniformity); a reduction in heterogeneous broadening in probe-molecule FTIR spectra for the freshly oxidized PdO/MgO sample is expected after its 700°C calcination. The narrower peak widths and therefore more differentiated contributions within each of the absorbing regions facilitated a more detailed assignment of FTIR spectral features. Supplementary adsorption experiments of two specific molecules (methyl formate and formaldehyde) were

Article



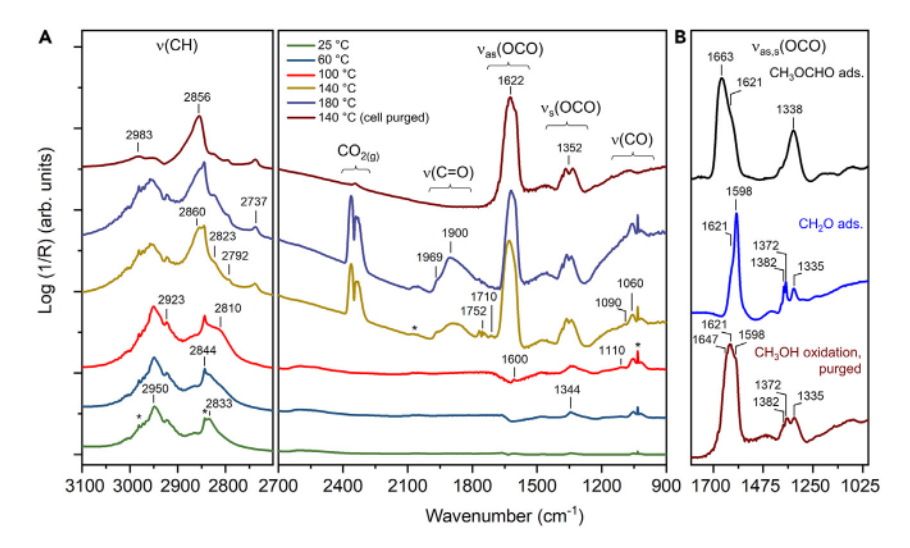


Figure 4. DRIFTS characterization of adsorbates on PdO/MgO

(A) Operando methanol oxidation measurements between 25°C and 180°C;  $p_{CH_3OH}/p_{O_2} = 1.45$ . \*Gas-phase methanol peak.

(B) Measurements recorded after He purge following  $CH_3OCHO$  adsorption,  $CH_2O$  adsorption, and methanol oxidation at 180°C.

conducted to aid the interpretation of spectra. The spectra of Figure 4B reflect methyl formate and formaldehyde adsorption at 180°C—that is, adsorption of two of the stable oxygenate products produced by methanol oxidation. This figure compares these spectra with a spectrum recorded after methanol oxidation experiments and purging the system of gas-phase reactants and products. The most notable observation from this comparison of direct oxygenate adsorption versus methanol oxidation catalysis is that they yield quite dissimilar intensity distributions within the peaks between 1,590 and 1,680 cm<sup>-1</sup>—those associated with the  $v_{as}(OCO)$  modes of surface-adsorbed formates. The clear variation among the  $v_s(OCO)$  modes (1,325–1,390 cm<sup>-1</sup>) further verifies these distinct adsorbate compositions. The signal for gas-phase methyl formate is centered at 1,752 cm<sup>-1</sup>; it is accompanied by a small additional feature at 1,710 cm<sup>-1</sup>, which we tentatively attribute to a physisorbed methyl formate that is in equilibrium with the gas phase since the wavenumber of the v(C=O) mode associated with this molecule is known to red shift upon adsorption.<sup>27</sup> The v(CH) region shows that as the temperature increases, the signal for surface methoxy (2,825-2,805 cm<sup>-1</sup>, asymmetric and symmetric CH<sub>3</sub> stretching modes of methoxy species<sup>25</sup>) first increases from 25°C to 100°C and then decreases. This decrease in the methoxy peak intensity is accompanied by a growth in that for surface formates (2,860 cm<sup>-1</sup>, CH stretching; 2,737 cm<sup>-1</sup>, a combination of the CH bending and OCO stretching frequencies of formates<sup>25,28</sup>), consistent with the appearance of  $v_{as}(OCO)$  peaks associated with formate, discussed above. This temperaturedependent evolution of peaks within the v(CH) region is expected and reflects the conversion of methanol to surface methoxy with oxidative conversion of surface methoxy to formate at higher temperatures.

It is apparent that formaldehyde adsorption generates a sharp peak at 1,598 cm $^{-1}$  with a shoulder at 1,621 cm $^{-1}$  (Figure 4B). Methyl formate adsorption at 180°C, in contrast, primarily generates  $v_{as}(OCO)$  peaks with the highest intensity centered at 1,663 cm $^{-1}$  and no clear contribution at 1,598 cm $^{-1}$ .



Surface formate		$\nu_{\text{as}}(\text{OCO})$
Chelating bidentate	H O = C     \    Mg - O	1598 cm <sup>-1</sup>
Bridging bidentate	H C O O Mg Mg	1621 cm <sup>-1</sup>
Monodentate	H O O O Mg	1647 cm <sup>-1</sup>

Scheme 1. Surface formate structures known to form on MgO surfaces
Assignments are based on observations from previous studies. 26,28,30–32

The narrow absorption peak centered at 1,598 cm $^{-1}$  generated from CH<sub>2</sub>O dosing is well known in the literature; it has been reported in many prior FTIR studies of CH<sub>2</sub>O adsorption and transformation on MgO surfaces. <sup>27,29–31</sup> Although intact CH<sub>2</sub>O molecules (or related polyoxomethylenes) adsorbed on MgO have been reported only at sub-ambient temperatures, <sup>32</sup> at room temperature and above, CH<sub>2</sub>O rapidly converts to a surface formate that is characterized by this  $v_{as}$ (OCO) absorption frequency. It is identified in the literature to correspond to a formate in a chelating bidentate configuration across Mg<sup>2+</sup>–O<sup>2-</sup> pairs<sup>31</sup> (see the discussion of Scheme 1 below).

On close examination of the temperature-dependent operando CH<sub>3</sub>OH oxidation DRIFTS spectra (Figure 4A), we observe that at low temperature (100°C) a narrow  $v_{as}(OCO)$  absorption mode appears near 1,600 cm $^{-1}$  without contributions from the modes at higher wavenumbers. The center frequency of this narrow feature is the same (within ca. 4 cm<sup>-1</sup>) as that due to the transformation of directly dosed formaldehyde on the surface, as noted above, and is therefore also assigned to chelating bidentate formate. The small shift in wavenumber here is attributable to an increased presence of H2O generated from the reaction, the electrondonating properties of which cause formate  $v_{as}(OCO)$  peaks to shift to lower wavenumbers. 26 Although at 100°C this feature is small, its assignment to a formate is supported by the concurrent appearance of the peak at 2,737 cm<sup>-1</sup> (shown magnified in Figure S5), which, as noted above, is uniquely assigned to a formate combination mode; this peak is also observed through formaldehyde adsorption (Figure S6). As will be shown below, this surface species is formed during methanol oxidation at the same temperature (100°C) at which C<sub>2</sub> product desorption commences. This observation, viewed in the context of proposals in prior methanol oxidation literature that formaldehyde is integral to C2 product formation,6 motivated our deeper analysis of this and other FTIR absorption features in the context of the catalysis.

**Article** 



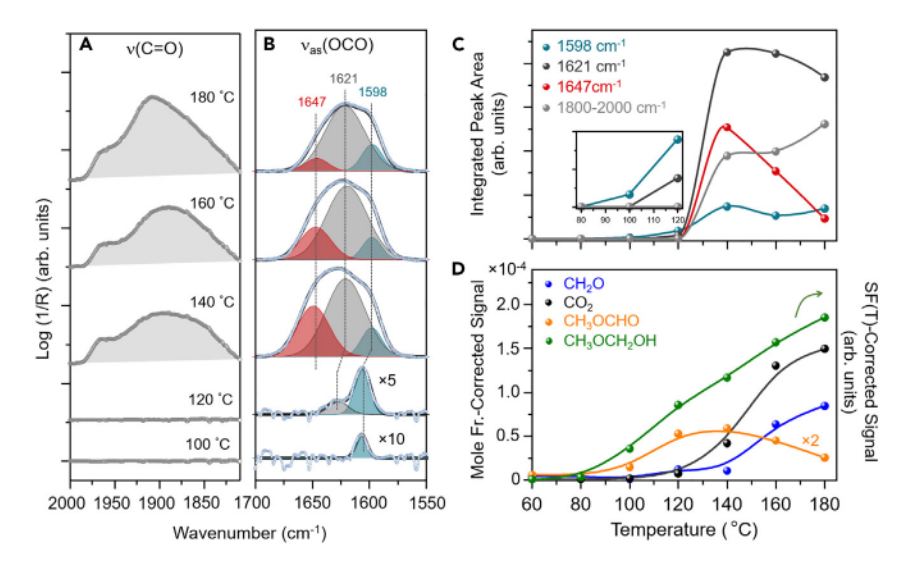


Figure 5. Analysis of temperature-dependent surface (DRIFTS) and near-surface (ns-MBMS) data for methanol oxidation catalysis with PdO/MgO

 $p_{CH_3OH}/p_{O_2} = 1.45.$ 

- (A) Magnification of  $\nu$ (C=O) absorption region.
- (B) Magnification of  $\nu_{as}(OCO)$  absorption region; peak deconvolution is shown.
- (C) Integrated intensities of absorption features from (A) and (B) are plotted with respect to temperature. Lines are added to guide the eyes.
- (D) ns-MBMS results (500 µm above surface) for products. Lines are added to guide the eyes.

The panels of Figure 5 reflect a simultaneous analysis of the temperature-dependent operando DRIFTS measurements and the signal intensities for product molecules measured by ns-MBMS at a position 500  $\mu m$  above the packed PdO/MgO surface. Figure 5A shows the intensities of the peaks from 1,800 to 2,000 cm<sup>-1</sup>, which are due to v(C=O) modes of Pd-CO species, at temperatures between 100°C and 180°C. Figure 5B shows the envelope  $v_{as}(OCO)$  absorption feature between 1,590 and 1,680 cm<sup>-1</sup>, resulting from surface formates, which was deconvolved into three peaks (see Scheme 1): the 1,598 cm<sup>-1</sup>-centered absorption band (chelating bidentate formate), which is dominant at low temperatures, and bands centered at 1,621 cm<sup>-1</sup> (bridging bidentate formate) and 1,647 cm<sup>-1</sup> (monodentate formate).<sup>26</sup> We integrated the intensities of these peaks, as well as those due to Pd-CO species, to qualitatively track their evolution with temperature. Figure 5C provides the temperature dependencies of these integrated DRIFTS peaks; the inset of this figure includes a magnification of the low-temperature region, which reflects the observation made above—that chelating bidentate formate first forms on the surface at 100°C.

When the temperature reached  $140^{\circ}\text{C}$  during the linear ramp, the intensities of the species discussed above (formates and carbonyls) were all found to rapidly increase; time-resolved spectra were recorded to capture this behavior (Figure S7). Above  $140^{\circ}\text{C}$ , with increasing temperature, the integrated intensity of the chelating bidentate formate peak is roughly constant, that of Pd–CO<sub>(s)</sub> increases, that of bridging bidentate formate gradually decreases, and that of monodentate formate rapidly decreases. The maximum concentration of surface monodentate formate is observed at  $140^{\circ}\text{C}$ .

Figure 5D provides ns-MBMS data for methanol oxidation with the PdO/MgO catalyst. This figure includes the reaction temperature dependencies of product species'

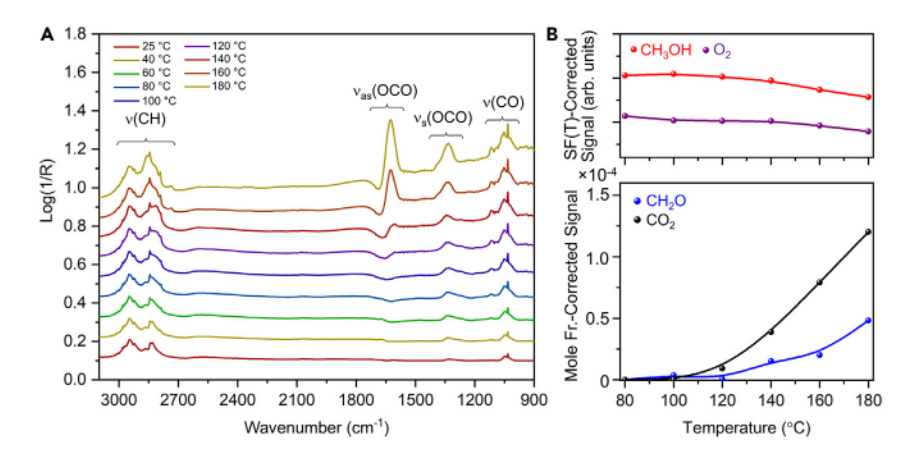


Figure 6. Operando surface and near-surface characterization of the pure MgO support during methanol oxidation

Spectra were recorded between 25°C and 180°C;  $p_{CH_3OH}/p_{O_2} = 1.45$ .

(A) DRIFTS results; spectral regions characteristic of major vibrational modes are labeled.

(B) ns-MBMS results (500 µm above surface) for reactants (top) and products (bottom).

integrated ion signals (with intensity correction and calibration applied, as in Figure 3B). The sampling nozzle was again positioned 500  $\mu m$  above the packed catalyst surface to record these data. The observed products and their associated lowest temperatures of observation were methoxymethanol, 100°C; methyl formate, 100°C; formaldehyde, 120°C; and CO<sub>2</sub>, 120°C. Therefore, at 100°C, methyl formate and methoxymethanol are the only carbon-containing products detected in the gas phase; the selectivity to C<sub>2</sub> oxygenates is 100% under this condition (within the sensitivity of the instrument,  $\sim\!1$  ppm).  $^{33}$  All product signals (except for that of methyl formate, which reaches its maximum near 140°C) increase as the temperature increases.

### The MgO support

Although non-oxidative thermal methanol decomposition has been examined over pure MgO in several studies, <sup>34,35</sup> to our knowledge, methanol oxidation using pure MgO catalysts has been reported only at a fixed temperature in a comprehensive overview of the reactivity of metal oxides for the reaction. <sup>36</sup> Figure 6 provides the temperature-dependent *operando* DRIFTS and ns-MBMS results for methanol oxidation over the bare MgO support. The DRIFTS spectra (Figure 6A) contain relatively broad absorption features, so detailed assignments are difficult, but it can be seen that methoxy (1,111 cm<sup>-1</sup>) readily forms on this surface at all temperatures, as expected and consistent with observations in the literature. <sup>37</sup> Surface formate is generated at about 140°C, a higher temperature than observed for Pd-PdO/MgO and PdO/MgO. This temperature coincides with that for initial detection of CO<sub>2</sub> and CH<sub>2</sub>O in the gas phase by ns-MBMS (Figure 6B).

### **DISCUSSION**

### PdO/MgO as a model system and the contrasting reactivities of PdO and O/Pd

The data in the results section show that PdO/MgO and Pd-PdO/MgO yield the same products when used to catalyze methanol oxidation. However, when PdO/MgO is used, the light-off temperatures of the  $C_1$  and  $C_2$  products are distinct: methyl formate and methoxymethanol are observed at  $100^{\circ}$ C and above, and  $CO_2$  and  $CO_2$  are observed at  $120^{\circ}$ C and above. For both Pd-PdO/MgO and PdO/MgO, the  $C_2$  species are produced concurrently. The results also show that

**Article** 



the PdO/MgO catalyst yields sharper and more differentiated adsorbate FTIR signatures than Pd-PdO/MgO, which facilitates absorption mode assignments, thereby enabling more precise identification of surface species. These observations highlight the utility of the oxidized sample, PdO/MgO, to serve as a model system for understanding the activity of Pd-based catalysts for methanol oxidation.

To frame the discussion and interpretation of our observations above, it is useful to outline relevant characteristics of MgO-supported Pd in the context of methanol oxidation catalysis. No  $C_2$  products are formed without the presence of Pd (Figure 6). In fact, Pd alone enables partial oxidations; unsupported PdO(101), <sup>38</sup> Pd(111), <sup>39</sup> and polycrystalline Pd films have been studied as methanol oxidation catalysts. Pd is commonly referred to as a "redox catalyst" because its oxidation state readily cycles between 2+ and 0, a characteristic that promotes surface-mediated oxidative dehydrogenations, as occurs to produce  $CH_2O$  from methanol.

The dynamics of the interconversion of Pd and PdO are complex and reaction dependent, and this interconversion is often integral to the activity of Pd as a catalyst component. 40 Catalytic combustion of methane is known to be especially sensitive to catalyst surface atomic structure and oxygen coordination around Pd. 41 For low-temperature selective oxidation of methanol to methyl formate, metallic Pd (or more precisely, chemisorbed oxygen on metallic Pd, notated as O/Pd) appears to be more active than PdO for the required oxidative dehydrogenation step. 21

MgO-supported Pd is often utilized as a model catalyst for fundamental studies <sup>25,42,43</sup> because it reflects the unique properties that emerge when a redox metal is coupled to a highly basic support. Although the irreducibility of MgO facilitates low concentrations of oxygen vacancies on the bare surface, it has been shown that energies for oxygen vacancy formation are greatly reduced at the interface between a Pd particle and the MgO surface. <sup>44</sup> The interface between Pd (or PdO) and MgO, and presumably specifically the local metal coordination environment within this region, appears to be essential to catalytic activity. For example, it has been reported that NO decomposition over Pd/MgO occurs through redox processes at sites comprising reduced Pd interacting with support Mg<sup>2+</sup>. <sup>45</sup>

Our prior work also highlights the important role of the Pd-support interaction in lowering energetic requirements for methanol oxidation: whereas Pd-PdO/MgO is here observed to catalyze C<sub>2</sub> product formation at as low as 40°C, unsupported Pd films do not generate these species in the near-surface gas phase below about 100°C for the same reactant feed ratio. That work with unsupported Pd and Au<sub>x</sub>Pd<sub>y</sub> alloys also showed the generation of a more diverse set of oxygenate products, including formic acid, dimethyl ether, acetaldehyde, and dimethoxymethane. If those species are produced here, they do not desorb and are apparently captured or converted by the MgO support in spillover events. It has been noted in a study of Pd/MgO catalysts that a cooperative effect occurs between the two phases: species produced on Pd surfaces spill over onto MgO, and the basic sites of MgO readily transform these species further. The product of the product

The results presented here reinforce the idea that the MgO support captures species generated at Pd surfaces and that the Pd–MgO interface is the active region for methanol oxidation catalysis. For example, the low-temperature (40°C) formation of near-surface methyl formate, methoxymethanol, and formaldehyde over the



# Chem Catalysis Article

Pd-PdO/MgO catalyst yields surface adsorbate FTIR signatures similar to those produced during higher temperature catalysis with the MgO alone. Our data suggest that the high activity of O/Pd (again, chemisorbed oxygen on metallic Pd domains present in this H<sub>2</sub>-reduced sample) rapidly produces molecules that are expected to be mobile on the metallic surface. Those products of oxidation that do not desorb from Pd are captured by the MgO support, except for CO, which expectedly binds strongly to Pd and yields the characteristic infrared absorptions of surface carbonyl. Methanol oxidation with the PdO/MgO catalyst most likely follows similar general mechanisms wherein reactions occur at Pd and Pd-MgO interface sites. During methanol oxidation, as the temperature increases, the surfaces of PdO particles are expected to form oxygen vacancies. The resultant PdO<sub>x</sub> contains undercoordinated Pd, providing sites for chemisorbed oxygen to efficiently dehydrogenate methanol and its oxidation products.

#### Constraining reaction mechanisms for methanol oxidation

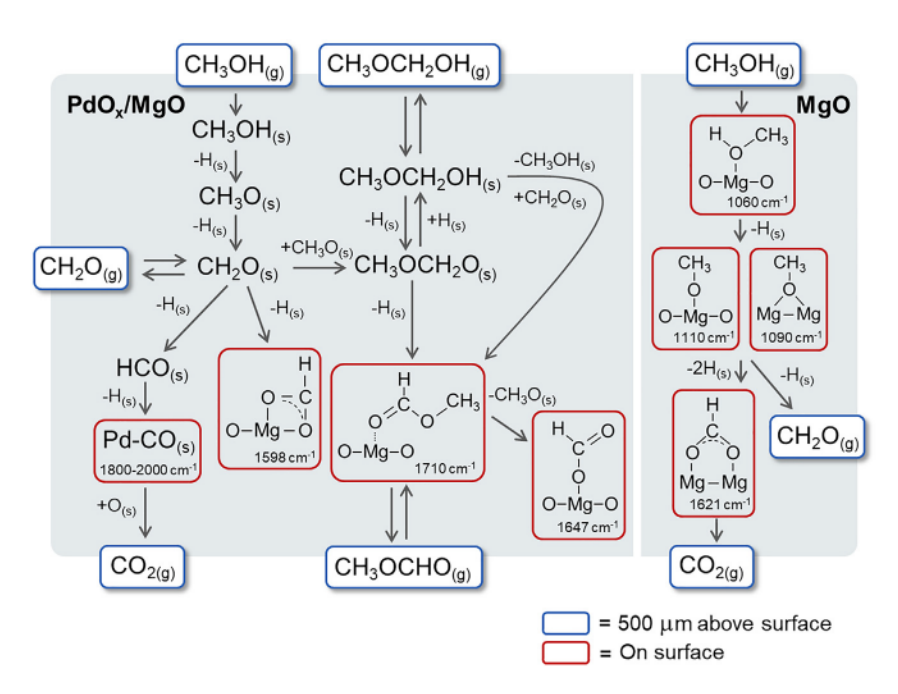
The most notable observations made regarding  $C_2$  species in this study of methanol oxidation with the PdO/MgO model catalyst are the following:

- (1) At the lowest temperature at which methoxymethanol and methyl formate are released to the near-surface gas phase—a condition where these are the only carbon-containing products desorbed—chelating bidentate formate appears on the surface. Stated another way, when C<sub>2</sub> product selectivity is 100%, chelating bidentate formate is the only oxygenate adsorbate observed on the surface (other than methoxy).
- (2) Chelating bidentate formate is the dominant surface-bound species formed when formaldehyde reacts with oxygen on the MgO surface.
- (3) As formaldehyde desorbs from the surface as a product of methanol oxidation at increasing rates, methyl formate desorbs at decreasing rates.
- (4) During temperature ramps, the concentrations of surface monodentate formate and gas-phase methyl formate initially increase and then decrease rapidly above 140°C.
- (5) Methanol oxidation with the MgO support alone yields only CO<sub>2</sub> and CH<sub>2</sub>O; production of C<sub>2</sub> products requires the presence of Pd or PdO.

When these and other observations from the ns-MBMS and DRIFTS measurements are taken together, a fairly complete picture of the reaction network can be derived. Scheme 2 shows the network implied by our observations, interpreted in the context of the vast literature on methanol oxidation and oxygenate adsorption on metal oxides. Species observed 500  $\mu m$  above the surface are outlined in blue, and surface-bound species are outlined in red.

The role of  $CH_2O$  in this network is prominent: its presence appears to be a requisite for the generation of methyl formate and methoxymethanol. The mechanism for their formation, commonly discussed in the related literature,  $^{46,47}$  first involves the surface coupling of  $CH_2O_{(s)}$  and  $CH_3O_{(s)}$ . This yields the adsorbed hemiacetal intermediate ( $CH_3OCH_2O_{(s)}$ ), which can be dehydrogenated to form methyl formate. Methyl formate desorbs and can re-adsorb, decomposing on the Pd/MgO surface at elevated temperatures. Because the signals for both gas-phase methyl formate and surface monodentate formate decrease rapidly above 140°C, the data provide evidence that surface monodentate formate is a product of methyl formate decomposition (which would result from cleavage of the ester oxygen–alkyl carbon bond across surface MgO pairs). If  $CH_3OCH_2O_{(s)}$  is hydrogenated, it forms methoxymethanol, which desorbs into the near-surface gas phase, from which it can re-adsorb on surfaces. On the catalyst





Scheme 2. Methanol oxidation reaction network implied by DRIFTS and ns-MBMS measurements

This scheme is derived from the current report's data, interpreted in the context of results from previous studies.  $^{21,46-51}$  The average wavenumbers for observed surface species are noted for reference. The entire diagram applies to PdO<sub>x</sub>/MgO catalysts, and the right-hand side applies to MgO. The temperature dependencies of steps are not reflected in the diagram, and interconversion among surface formates is omitted.

surface, it can be oxidatively dehydrogenated to form methyl formate, or it could transfer an H atom to  $\text{CH}_2\text{O}_{(s)}$ , forming methyl formate and releasing  $\text{CH}_3\text{O}_{(s)}$ . Some evidence for this second pathway might exist in the temperature-dependent ns-MBMS data in Figures 3 and 5. Whereas an increased rate of formaldehyde desorption correlates negatively with that of methyl formate desorption, it correlates positively with that of methoxymethanol desorption. This could suggest that reaction of methoxymethanol with formaldehyde on surfaces tends to reduce the steady-state concentration of near-surface gas-phase methoxymethanol. Although these noted features of the temperature-dependent data alone are insufficient to determine the degree to which this step is operable here, it is likely that some fraction of methyl formate forms through the methoxymethanol intermediate.

In a prior methanol oxidation study using  $Pd/Al_2O_3$ , under conditions where high methyl formate selectivity was achieved, the absence of detectable formaldehyde in the reactor effluent was said to indicate that it very rapidly reacts on the surface with  $CH_3O_{(s)}$ . <sup>21</sup> In a methanol oxidation study of silica-supported Mo catalysts, when methyl formate generation was observed in the absence of gas-phase formaldehyde, it was suggested that desorption of formaldehyde was more energetically demanding than its spillover onto silica and that the silica sites were essential to the chemistry <sup>51</sup>; an increase in formaldehyde desorption and concomitant decrease in methyl formate production was found at elevated temperatures in that study, as seen in our data. We deduce it is also true for PdO/MgO that surface formaldehyde is present at low temperatures where  $C_2$  selectivity is 100%. We suggest, on the basis of the analysis of FTIR spectra provided above, that its presence on the catalyst surface in that condition is indirectly indicated through the isolated chelating bidentate formate  $v_{as}(OCO)$  absorption mode, which serves as a finger-print of  $CH_2O^{29-32}$  that has spilled over onto the support:



$$CH_3O_{(s)} + O_{(s)} \xrightarrow{Pd} CH_2O_{(s)} + OH_{(s)} \tag{Equation 1}$$

$$CH_2O_{(s)} + O_{(s)} \xrightarrow{MgO} O = C + OH_{(s)}$$

$$Mq - O$$
(Equation 2A)

$$CH_2O_{(s)} + CH_3O_{(s)} + H_{(s)} \rightarrow CH_3OCH_2OH_{(s)} \rightarrow CH_3OCH_2OH_{(g)} \qquad \text{(Equation 2B)}$$

Equation 1 describes the oxidative dehydrogenation of methoxy at Pd sites to generate surface-bound formaldehyde. Equations 2A and 2B describe the competing pathways for subsequent transformation of formaldehyde: the spillover onto the MgO support (Equation 2A) and the surface-mediated coupling events resulting in the formation and subsequent desorption of methoxymethanol to the near-surface gas phase (Equation 2B). The key supporting information for these claims lies in the molecular structure of methoxymethanol (H<sub>3</sub>C–O–CH<sub>2</sub>–O–H), which forms concurrently with formaldehyde. The presence of the dioxymethylene group (O–CH<sub>2</sub>–O) in this molecule requires that a methylene-containing intermediate be involved in the coupling event from which it originates. An alternative pathway for C<sub>2</sub> product formation involves reactions of surface formates with methanol<sup>52</sup>; if this were the primary pathway here, the dioxymethylene group would not be found in the gas-phase intermediate over the entire temperature range.

### Conclusions

In this study, we combined ns-MBMS and surface-sensitive operando DRIFTS to investigate the origins of C2 oxygenates from methanol oxidation catalysis at atmospheric pressure with the use of MgO-supported Pd. Analysis emphasized results from oxidized PdO/MgO, which predominantly contains Pd<sup>2+</sup>. Here, detection of reactive methoxymethanol in the near-surface gas phase was uniquely possible through ns-MBMS measurements using a small-aperture nozzle probe close to the surface, which minimized the probability of collisions with catalyst surfaces, reactor walls, or other molecules prior to its detection in the time-of-flight mass spectrometer. One of our most important observations is that whereas the catalyst surface is populated with methoxy and formate in an adsorption configuration involving surface Mg<sup>2+</sup>-O<sup>2-</sup> pairs under reaction conditions associated with 100% selectivity to C<sub>2</sub> products (methyl formate and methoxymethanol), the presence of the dioxymethylene (O-CH2-O) group in near-surface methoxymethanol requires that formaldehyde, undetected on the surface but transiently present, be a primary building block of these desorbing C2 oxygenates. In this way, analysis of the near-surface gas phase served to constrain the interpretation of the roles of adsorbates and, therefore, the overall reaction mechanism, for methanol oxidation.

### **EXPERIMENTAL PROCEDURES**

#### Resource availability

### Lead contact

Requests for further information and resources should be directed to and will be fulfilled by the lead contact, Coleman Kronawitter (ckrona@ucdavis.edu).

### Materials availability

Material preparation is described in the supplemental information.

### Article



### Data and code availability

Any additional information needed for analyzing the data is available from the lead contact upon request. No code was generated.

#### Methods

Experimental details are provided in the supplemental information.

### SUPPLEMENTAL INFORMATION

Supplemental information can be found online at https://doi.org/10.1016/j.checat. 2023.100782.

#### **ACKNOWLEDGMENTS**

C.X.K., S.M.G., and L.R.F. acknowledge support from the Gas-Phase Chemical Physics (GPCP) and Catalysis Science programs of the Chemical Sciences, Geosciences, and Biosciences (CSGB) Division of the US Department of Energy (DOE) Basic Energy Sciences (BES) program under grant DE-SC0020320. D.L.O., N.H., J.H.F., and C.X.K. acknowledge support from DOE-BES-CSGB FWP grant 021507 for contributions related to technique development. S.M.G. and L.R.F. acknowledge Sandia's Campus Executive LDRD program for supporting research at the Combustion Research Facility. XPS measurements were made possible by National Science Foundation (NSF) grant MRI-1828238. K.v.B. acknowledges NSF-DMR-1836571 for TEM characterization. Sandia National Laboratories is a multimission laboratory managed and operated by National Technology and Engineering Solutions of Sandia LLC, a wholly owned subsidiary of Honeywell International Inc. for the US DOE's National Nuclear Security Administration under contract DENA0003525. This paper describes objective technical results and analysis. Any subjective views or opinions that might be expressed in the paper do not necessarily represent the views of the US DOE or the US government.

### **AUTHOR CONTRIBUTIONS**

S.M.G. co-designed the study and designed and executed experiments; N.F. assisted with DRIFTS setup and experiments; L.R.F. performed XPS measurements; A.J.Z. assisted with the operation and maintenance of the MBMS system; J.W. and K.v.B. recorded and analyzed the TEM data; J.H.F., N.H., and D.L.O. supervised all aspects of the near-surface gas-phase measurements; C.X.K. co-designed the study and supervised; all authors participated in the editing and revision of the manuscript.

### **DECLARATION OF INTERESTS**

The authors declare no competing interests.

Received: June 27, 2023 Revised: September 25, 2023 Accepted: September 26, 2023 Published: October 19, 2023

#### REFERENCES

- Chakrabarti, A., Ford, M.E., Gregory, D., Hu, R., Keturakis, C.J., Lwin, S., Tang, Y., Yang, Z., Zhu, M., Bañares, M.A., and Wachs, I.E. (2017). A decade+ of operando spectroscopy studies. Catal. Today 283, 27–53. https://doi.org/10. 1016/J.CATTOD.2016.12.012.
- Zaera, F. (2021). In-situ and operando spectroscopies for the characterization of catalysts and of mechanisms of catalytic reactions. J. Catal. 404, 900–910. https://doi.org/10.1016/J.JCAT. 2021.08.013.
- Anderson, L.C., Xu, M., Mooney, C.E., Rosynek, M.P., and Lunsford, J.H. (1993). Hydroxyl radical formation during the reaction of oxygen with methane or water over basic lanthanide oxide catalysts. J. Am. Chem. Soc. 115, 6322– 6326. https://doi.org/10.1021/JA00067A055.



- Takanabe, K., and Iglesia, E. (2008). Rate and selectivity enhancements mediated by OH radicals in the oxidative coupling of methane catalyzed by Mn/Na<sub>2</sub>WO<sub>4</sub>/SiO<sub>2</sub>. Angew. Chem. 120, 7803–7807. https://doi.org/10. 1002/ANGE.200802608.
- Steinmetz, S.A., DeLaRiva, A.T., Riley, C., Schrader, P., Datye, A., Spoerke, E.D., and Kliewer, C.J. (2022). Gas-phase hydrogen-atom measurement above catalytic and noncatalytic materials during ethane dehydrogenation. J. Phys. Chem. C 126, 3054–3059. https://doi. org/10.1021/ACS.JPCC.1C09955.
- Gurses, S.M., Price, T., Zhang, A., Frank, J.H., Hansen, N., Osborn, D.L., Kulkarni, A., and Kronawitter, C.X. (2021). Near-surface gasphase methoxymethanol is generated by methanol oxidation over Pd-based catalysts. J. Phys. Chem. Lett. 12, 11252–11258. https://doi.org/10.1021/ACS.JPCLETT. 1C03381.
- Zhou, B., Huang, E., Almeida, R., Gurses, S., Ungar, A., Zetterberg, J., Kulkarni, A., Kronawitter, C.X., Osborn, D.L., Hansen, N., and Frank, J.H. (2021). Near-surface imaging of the multicomponent gas phase above a silver catalyst during partial oxidation of methanol. ACS Catal. 11, 155–168. https://doi.org/10. 1021/ACSCATAL.0C04396.
- Pfaff, S., Rämisch, L., Gericke, S.M., Larsson, A., Lundgren, E., and Zetterberg, J. (2022). Visualizing the gas diffusion induced ignition of a catalytic reaction. ACS Catal. 12, 6589– 6595. https://doi.org/10.1021/ACSCATAL. 2C01666.
- Wan, S., Torkashvand, B., Häber, T., Suntz, R., and Deutschmann, O. (2020). Investigation of HCHO catalytic oxidation over platinum using planar laser-induced fluorescence. Appl. Catal., B 264, 118473. https://doi.org/10.1016/ J.APCATB.2019.118473.
- McGuire, N.E., Sullivan, N.P., Deutschmann, O., Zhu, H., and Kee, R.J. (2011). Dry reforming of methane in a stagnation-flow reactor using Rh supported on strontium-substituted hexaaluminate. Appl. Catal. Gen. 394, 257–265. https://doi.org/10.1016/J.APCATA.2011. 01.009.
- Moshammer, K., Jasper, A.W., Popolan-Vaida, D.M., Lucassen, A., Diévart, P., Selim, H., Eskola, A.J., Taatjes, C.A., Leone, S.R., Sarathy, S.M., et al. (2015). Detection and identification of the keto-hydroperoxide (HOOCH2OCHO) and other intermediates during lowtemperature oxidation of dimethyl ether. J. Phys. Chem. A 119, 7361–7374. https://doi. org/10.1021/ACS.JPCA.5B00101.
- Barr, T.L. (1978). An ESCA study of the termination of the passivation of elemental metals. J. Phys. Chem. 82, 1801–1810. https:// doi.org/10.1021/J100505A006.
- Légaré, P., Finck, F., Roche, R., and Maire, G. (1989). XPS investigation of the oxidation of the Al/Pd interface: the Al<sub>2</sub>O<sub>3</sub>/Pd interface. Surf. Sci. 217, 167–178. https://doi.org/10.1016/ 0039-6028(89)90542-6.
- Weerachawanasak, P., Hutchings, G.J., Edwards, J.K., Kondrat, S.A., Miedziak, P.J., Prasertham, P., and Panpranot, J. (2015). Surface functionalized TiO<sub>2</sub> supported Pd catalysts for solvent-free selective oxidation of

- benzyl alcohol. Catal. Today 250, 218–225. https://doi.org/10.1016/J.CATTOD.2014.
- Kibis, L.S., Titkov, A.I., Stadnichenko, A.I., Koscheev, S.V., and Boronin, A.I. (2009). X-ray photoelectron spectroscopy study of Pd oxidation by RF discharge in oxygen. Appl. Suff. Sci. 255, 9248–9254. https://doi.org/10. 1016/J.APSUSC.2009.07.011.
- Kibis, L.S., Stadnichenko, A.I., Koscheev, S.V., Zaikovskii, V.I., and Boronin, A.I. (2012). Highly oxidized palladium nanoparticles comprising Pd<sup>4+</sup> species: spectroscopic and structural aspects, thermal stability, and reactivity. J. Phys. Chem. C 116, 19342–19348. https://doi. org/10.1021/jp305166k.
- Nolte, P., Stierle, A., Balmes, O., Srot, V., van Aken, P.A., Jeurgens, L.P.H., and Dosch, H. (2009). Carbon incorporation and deactivation of MgO(001) supported Pd nanoparticles during CO oxidation. Catal. Today 145, 243–250. https://doi.org/10.1016/J.CATTOD. 2008.12.002.
- Lupan, O., Postica, V., Hoppe, M., Wolff, N., Polonskyi, O., Pauporté, T., Viana, B., Majérus, O., Kienle, L., Faupel, F., and Adelung, R. (2018). PdO/PdO<sub>2</sub> functionalized ZnO:::Pd films for lower operating temperature H<sub>2</sub> gas sensing. Nanoscale 10, 14107–14127. https:// doi.org/10.1039/c8nr03260b.
- Tu, W., and Chin, Y.H.C. (2015). Catalytic consequences of chemisorbed oxygen during methanol oxidative dehydrogenation on Pd clusters. ACS Catal. 5, 3375–3386. https://doi. org/10.1021/ACSCATAL.5B00068.
- Wojcieszak, R., Gaigneaux, E.M., and Ruiz, P. (2012). Low temperature-high selectivity process over supported Pd nanoparticles in partial oxidation of methanol. ChemCatChem 4, 72–75. https://doi.org/10.1002/CCTC. 201100215.
- Lichtenberger, J., Lee, D., and Iglesia, E. (2007). Catalytic oxidation of methanol on Pd metal and oxide clusters at near-ambient temperatures. Phys. Chem. Chem. Phys. 9, 4902–4906. https://doi.org/10.1039/ B707465D.
- Busca, G. (1996). Infrared studies of the reactive adsorption of organic molecules over metal oxides and of the mechanisms of their heterogeneously-catalyzed oxidation. Catal. Today 27, 457–496. https://doi.org/10.1016/ 0920-5861(95)00162-X.
- Burcham, L.J., Briand, L.E., and Wachs, I.E. (2001). Quantification of active sites for the determination of methanol oxidation turn-over frequencies using methanol chemisorption and in situ infrared techniques. 1. Supported metal oxide catalysts. Langmuir 17, 6164–6174. https://doi.org/10.1021/LA010009U.
- Gyngazova, M.S., Grazia, L., Lolli, A., Innocenti, G., Tabanelli, T., Mella, M., Albonetti, S., and Cavani, F. (2019). Mechanistic insights into the catalytic transfer hydrogenation of furfural with methanol and alkaline earth oxides. J. Catal. 372, 61–73. https://doi.org/10.1016/J.JCAT. 2019.02.020.
- Bertarione, S., Scarano, D., Zecchina, A., Johánek, V., Hoffmann, J., Schauermann, S., Libuda, J., Rupprechter, G., and Freund, H.-J.

- (2004). Surface reactivity of Pd nanoparticles supported on polycrystalline substrates as compared to thin film model catalysts: infrared study of CH<sub>3</sub>OH adsorption. J. Catal. 223, 64–73. https://doi.org/10.1016/J.JCAT.2004. 01.005.
- Shido, T., Asakura, K., and Iwasawa, Y. (1990). Reactant-promoted reaction mechanism for catalytic water-gas shift reaction on MgO. J. Catal. 122, 55–67. https://doi.org/10.1016/ 0021-9517(90)90261-H.
- Chuang, C.-C., Wu, W.-C., Huang, M.-C., Huang, I.-C., and Lin, J.-L. (1999). FTIR study of adsorption and reactions of methyl formate on powdered TiO<sub>2</sub>. J. Catal. 185, 423–434. https:// doi.org/10.1006/JCAT.1999.2516.
- Martin, C., Martin, I., and Rives, V. (1992). An FT-IR study of the adsorption of pyridine, formic acid and acetic acid on magnesia and molybdena-magnesia. J. Mol. Catal. 73, 51–63. https://doi.org/10.1016/0304-5102(92) 80061-K.
- Wang, G.-W., Hattori, H., Itoh, H., and Tanabe, K. (1982). The formation of adsorbed formaldehyde by the reaction of adsorbed carbon monoxide with hydrogen on magnesium oxide. J. Chem. Soc. Chem. Commun. 1256–1257. https://doi.org/10.1039/ C39820001256.
- Wang, G.-W., and Hattori, H. (1984). Reaction of adsorbed carbon monoxide with hydrogen on magnesium oxide. J. Chem. Soc., Faraday Trans. 1 80, 1039–1047. https://doi.org/10. 1039/F19848001039.
- Kohno, Y., Ishikawa, H., Tanaka, T., Funabiki, T., and Yoshida, S. (2001). Photoreduction of carbon dioxide by hydrogen over magnesium oxide. Phys. Chem. Chem. Phys. 3, 1108–1113. https://doi.org/10.1039/B008887K.
- Busca, G., Lamotte, J., Lavalley, J.-C., and Lorenzelli, V. (1987). FT-IR study of the adsorption and transformation of formaldehyde on oxide surfaces. J. Am. Chem. Soc. 109, 5197–5202. https://doi.org/10.1021/ JA00251A025.
- Ruwe, L., Moshammer, K., Hansen, N., and Kohse-Höinghaus, K. (2018). Influences of the molecular fuel structure on combustion reactions towards soot precursors in selected alkane and alkene flames. Phys. Chem. Chem. Phys. 20, 10780–10795. https://doi.org/10. 1039/C7CP07743B.
- Foyt, D., and White, J.M. (1977). Thermal decomposition of methanol adsorbed on magnesia. J. Catal. 47, 260–268. https://doi. org/10.1016/0021-9517(77)90173-7.
- Hu, J., Zhu, K., Chen, L., Kübel, C., and Richards, R. (2007). MgO(111) nanosheets with unusual surface activity. J. Phys. Chem. C 111, 12038–12044. https://doi.org/10.1021/ JP073383X.
- Badlani, M., and Wachs, I.E. (2001). Methanol: a "smart" chemical probe molecule. Catal. Lett. 75, 137–149. https://doi.org/10.1023/ A:1016715520904.
- Bensitel, M., Saur, O., and Lavalley, J.C. (1991). Use of methanol as a probe to study the adsorption sites of different MgO samples. Mater. Chem. Phys. 28, 309–320. https://doi. org/10.1016/0254-0584(91)90086-A.

### **Article**



- Hakanoglu, C., Hinojosa, J.A., and Weaver, J.F. (2011). Oxidation of methanol on a PdO(101) thin film. J. Phys. Chem. C 115, 11575–11585. https://doi.org/10.1021/JP201623A.
- Borasio, M., Rodríguez de la Fuente, O., Rupprechter, G., and Freund, H.-J. (2005). In situ studies of methanol decomposition and oxidation on Pd(111) by PM-IRAS and XPS spectroscopy. J. Phys. Chem. B 109, 17791–17794. https://doi.org/10.1021/ JP053855C.
- Chin, Y.H.C., García-Diéguez, M., and Iglesia, E. (2016). Dynamics and thermodynamics of Pd-PdO phase transitions: effects of Pd cluster size and kinetic implications for catalytic methane combustion. J. Phys. Chem. C 120, 1446–1460. https://doi.org/10.1021/ACS. JPCC.5806677.
- Hellman, A., Resta, A., Martin, N.M., Gustafson, J., Trinchero, A., Carlsson, P.-A., Balmes, O., Felici, R., van Rijn, R., Frenken, J.W.M., et al. (2012). The active phase of palladium during methane oxidation. J. Phys. Chem. Lett. 3, 678–682. https://doi.org/10.1021/JZ300069S.
- Abbet, S., Ferrari, A.M., Giordano, L., Pacchioni, G., Häkkinen, H., Landman, U., and Heiz, U. (2002). Pd1/MgO(100): a model system in nanocatalysis. Surf. Sci. 514, 249–255. https://doi.org/10.1016/S0039-6028(02) 01637-0.

- Matveev, A.V., M Neyman, K., Pacchioni, G., and Rösch, N. (1999). Density functional study of M4 clusters (M=Cu, Ag, Ni, Pd) deposited on the regular MgO(001) surface. Chem. Phys. Lett. 299, 603–612. https://doi.org/10.1016/ S0009-2614(98)01183-X.
- Giordano, L., Goniakowski, J., and Pacchioni, G. (2001). Characteristics of Pd adsorption on the MgO surface: role of oxygen vacancies. Phys. Rev. B 64, 075417. https://doi.org/10. 1103/PhysRevB.64.075417.
- Ogata, A., Obuchi, A., Mizuno, K., Ohi, A., and Ohuchi, H. (1993). Active sites and redox properties of supported palladium catalysts for nitric oxide direct decomposition. J. Catal. 144, 452-459. https://doi.org/10.1006/JCAT. 1993.1345.
- Wachs, I.E., and Madix, R.J. (1978). The oxidation of methanol on a silver (110) catalyst. Surf. Sci. 76, 531–558. https://doi.org/10.1016/ 0039-6028(78)90113-9.
- Liu, H.X., Zhang, R.S., Yao, X.J., Liu, M.C., Hu, Z.D., and Fan, B.T. (2004). Effects of support on bifunctional methanol oxidation pathways catalyzed by polyoxometallate Keggin clusters. J. Catal. 44, 161–167. https://doi.org/10.1016/ JJCAT.2004.01.012.
- Stowers, K.J., Madix, R.J., and Friend, C.M. (2013). From model studies on Au(111) to

- working conditions with unsupported nanoporous gold catalysts: oxygen-assisted coupling reactions. J. Catal. 308, 131–141. https://doi.org/10.1016/J.JCAT. 2013.05.033.
- Akuri, S.R., Dhoke, C., Rakesh, K., Hegde, S., Nair, S.A., Deshpande, R., and Manikandan, P. (2017). Decomposition of methyl formate over supported Pd catalysts. Catal. Lett. 147, 1285– 1293. https://doi.org/10.1007/S10562-017-2011-y.
- Takahashi, K., Takezawa, N., and Kobayashi, H. (1983). Mechanism of formation of methyl formate from formaldehyde over copper catalysts. Chem. Lett. 12, 1061–1064. https://doi.org/10.1246/CL. 1983.1061.
- Louis, C., Tatibouët, J.-M., and Che, M. (1988). Catalytic properties of silica-supported molybdenum catalysts in methanol oxidation: the influence of molybdenum dispersion.
   J. Catal. 109, 354–366. https://doi.org/10.1016/ 0021-9517(88)90218-7.
- Sambeth, J., Juan, A., Gambaro, L., and Thomas, H. (1997). Catalytic oxidation of CH<sub>3</sub>OH to HCOOCH<sub>3</sub> on V<sub>2</sub>O<sub>5</sub>: a theoretical study. J. Mol. Catal. Chem. 118, 283–291. https://doi.org/10.1016/S1381-1169(96) 00900-4.